



Evolutionary computing methodology for small wind turbine supporting structures

Jakub Bukala¹ · Krzysztof Damaziak¹ · Hamid Reza Karimi² · Jerzy Malachowski¹ · Kjell Gunnar Robbersmyr³

Received: 25 June 2018 / Accepted: 4 October 2018 / Published online: 20 October 2018
© The Author(s) 2018

Abstract

The paper presents a comprehensive, complex, numerical, optimization methodology (computational framework) dedicated for supporting structures of small-scale wind turbines. The small wind turbine (SWT) supporting structure is one of the key components determining the cost of such a device. Therefore, the supporting structure optimization will allow cost reduction and, hence, popularization of these devices around the world. The presented methodology is based on the following: single-objective (aggregation-approach to multi-objective problem) evolutionary algorithm driven optimization, finite-element structural analyses, estimation of wind energy capture efficiency (coupled aero-servo-elastic numerical simulations), and economic evaluation (based on real meteorological data). Then, the methodology is proposed for a guy-wired mast structure of an arbitrary chosen SWT model. The optimization of chosen design features of the structure is performed and as a result the optimal solution for given assumptions is presented and scaling factor for that case is identified (total mass of the foundations). The successful use of combined numerical methods (genetic algorithms, FE method analyses, coupled aero-servo-elastic numerical simulations, pre-/post-processing scripts, and economic evaluation models) is the main novelty of this work.

Keywords Small wind turbine · Optimization · Finite element method · Genetic algorithm · Evolutionary algorithm

1 Introduction

The field of eco-energy production has high expectations for the development and dissemination of small wind turbines

✉ Jerzy Malachowski
jerzy.malachowski@wat.edu.pl

Jakub Bukala
jakub.bukala@wat.edu.pl

Krzysztof Damaziak
krzysztof.damaziak@wat.edu.pl

Hamid Reza Karimi
hamidreza.karimi@polimi.it

Kjell Gunnar Robbersmyr
kjell.g.robbersmyr@uia.no

¹ Department of Mechanics and Applied Computer Science, Faculty of Mechanical Engineering, Military University of Technology, Gen. Witolda Urbanowicza 2, 00-908 Warsaw, Poland

² Department of Mechanical Engineering, Politecnico di Milano, Via Giuseppe La Masa, 1, 20156 Milan, Italy

³ Department of Engineering Sciences, University of Agder, Jon Lilletunsvet 9, Grimstad, Norway

(SWTs). Without the dissemination of SWTs, fulfilling legal requirements for energy efficiency and energy production from renewable sources may be difficult [1]. The wide prevalence of SWTs and the emergence of so-called prosumers in the electrical grid (the Smart Grid concept) are among the most important factors that will change the way power companies deliver service over the next decade [2].

According to the IEC 61400-2 standard, SWTs have a rotor area and rated power of less than 200 m² and 50 kW, respectively [3]. Wind power plants in this category are generally designed for small and individual customers, such as households, farms, weather stations, and road signalization. The global number of operating SWTs is increasing at an annual rate of 8%, and at the end of 2013, the total number of SWTs worldwide was approximately 870,000 [1].

SWT profitability is a function of turbine efficiency, cost, and reliability [4]. These features in turn depend on SWT design and applied technical solutions. A key SWT component is the supporting structure. Utility-scale wind turbine towers are mostly tubular. Although tubular-type towers are commonly used in SWT installations, guyed lattice masts are also used. Guy-wired masts are less expensive and lighter than tubular towers and are capable of providing sufficient support

for SWTs [5]. The tilt-up poles/towers are very popular since they are easy to install and offer good accessibility for maintenance and repair [5].

The SWT supporting structure is responsible for approximately 20–25% of the total SWT installation cost [5]. Therefore, optimizing the mast design both in terms of cost reduction and annual energy production will further promote the popularization of these devices around the world, with significant, positive impacts on eco-energy production.

The term optimization refers to the finding of feasible solutions which correspond to extreme values of one or multiple objectives [6]. However, optimization of the design of wind turbine is not a straightforward task (the wide variety of possible parameters as well as the complex characteristics of the external factors influencing their operation) and often requires innovative techniques and algorithms [7].

There are many algorithms that can be gradient-based or heuristic-based that solves single-objective optimization problems. Besides deterministic search techniques, there are stochastic search algorithms that seek to find the global optimal solution with more ease [8]. Among them, evolutionary algorithms (EAs) mimic nature's evolutionary principles and are now emerging as popular algorithms to solve complex optimization problems [9].

In order to perform the optimization procedure, a computational framework (or an optimization methodology) is needed to ensure the correct data exchange and efficient communication between particular modules [10]. The methodology under consideration should consider all key factors of turbine operation, such as the coupled aerodynamic-structural responses of the structure, estimated energy production under the given conditions, and all real-world restrictions. Therefore, a multi-objective optimization (MOO), where many objectives are considered, is indispensable [11]. Moreover, the methodology should be focused on SWTs and allow simple and robust calculations regardless of the input data. Such assumptions favor simple and proven approaches over sophisticated, niche solutions.

Previous reviews of the literature on wind turbine optimization [12, 13] have focused on the optimization of utility-scale wind turbines rather than SWTs. In many works, wind turbine tower optimization for utility-scale wind turbines is discussed [14–20]. This also applies to wind turbine blade optimization for utility-scale wind turbines [21–26].

By contrast, the literature of SWTs have focused mainly on partial, isolated solutions, such as structural blade optimization [27–31] or controlling systems optimization [32–34]. In several papers, the main focus is put on specific design solutions, such as vertical axis wind turbines [35–37]. The few works that have examined the optimization of the supporting structures of SWTs [38] have not included an economic evaluation in their methodology, and thus there is a significant possibility that the optimal structural solutions obtained using

these methodologies are counterfeit in terms of overall economy (manufacturing costs, installation costs, maintenance costs, etc. [5]).

After careful review of previous researches, it has been summarized that the literature related to complex optimization of SWT supporting structures with structural analysis, wind energy capture efficiency, and economic evaluation is scanty. Therefore, a computational framework for optimization of SWT supporting structures has been developed using evolutionary algorithm. The proposed methodology is focused on cost, effectiveness, flexibility, and reliability aspects.

2 Methodology

The presented methodology relies on a specific combination of relatively simple and proven technical approaches for solving specific aspects, such as single-objective evolutionary algorithm driven optimization (aggregation-approach to MOO), finite-element structural analyses, estimation of wind energy capture efficiency (coupled aero-servo-elastic numerical simulations), and economic evaluation (based on meteorological data). The chosen algorithms are integrated to allow mutual data exchange (coupled solution) and automatically lead to an optimal solution after provision of the required input data.

2.1 Optimization strategy

The optimization objective in the presented methodology is to minimize the payback period (PP) with respect to the computed mass of the construction and estimated energy production in a given period. In this case, multi-objective optimization is transformed to a single-objective optimization (SOO) problem by using an a priori given scalarization function and a priori given weights and constraints (aggregation-approach to MOO in order to find Pareto-optimal solution) [39]. Therefore, the optimization problem can be formulated as follows:

$$\begin{aligned} & \min PP_j(x_{1j}, x_{2j}, x_{3j}, \dots, x_{nj}) \\ \text{subject to } & \sigma_{xj}(x_{1j}, x_{2j}, x_{3j}, \dots, x_{nj}) < \sigma_{x_max} \\ & b_{xj}(x_{1j}, x_{2j}, x_{3j}, \dots, x_{nj}) > b_{x_min} \end{aligned} \quad (1)$$

where PP_j is the PP of variant j [years], x_{nj} are variant j optimization variables, σ_{xj} is the variant j stress response, b_{xj} is the variant j structural buckling response, σ_{x_max} is the assumed stress limit, and b_{x_min} is the assumed buckling limit.

The optimization procedure is performed in repeatable cycles (the optimization loop). In each cycle, a set of individual components provides a solution for a particular step owning to mutual data exchange. A schematic overview of the procedure is presented in Fig. 1.

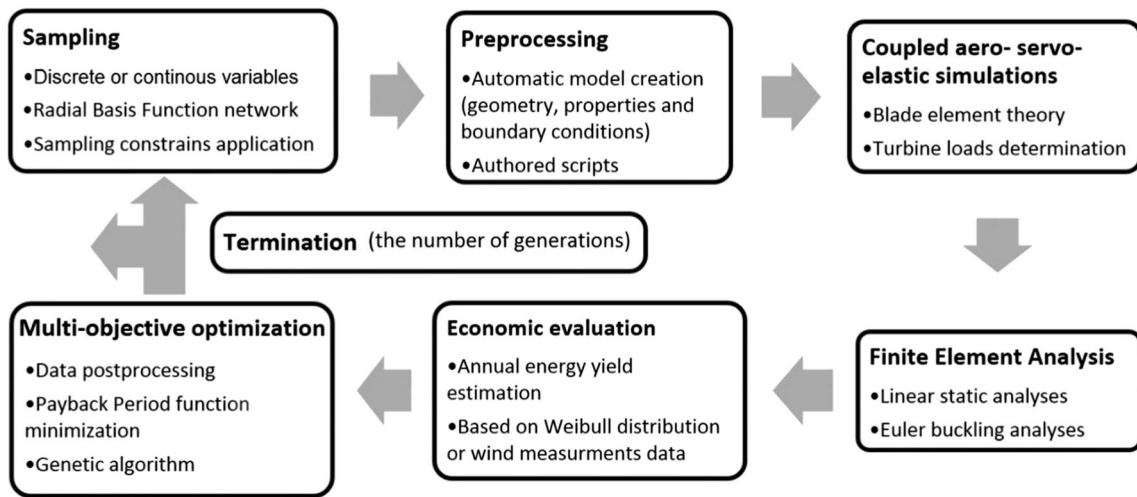


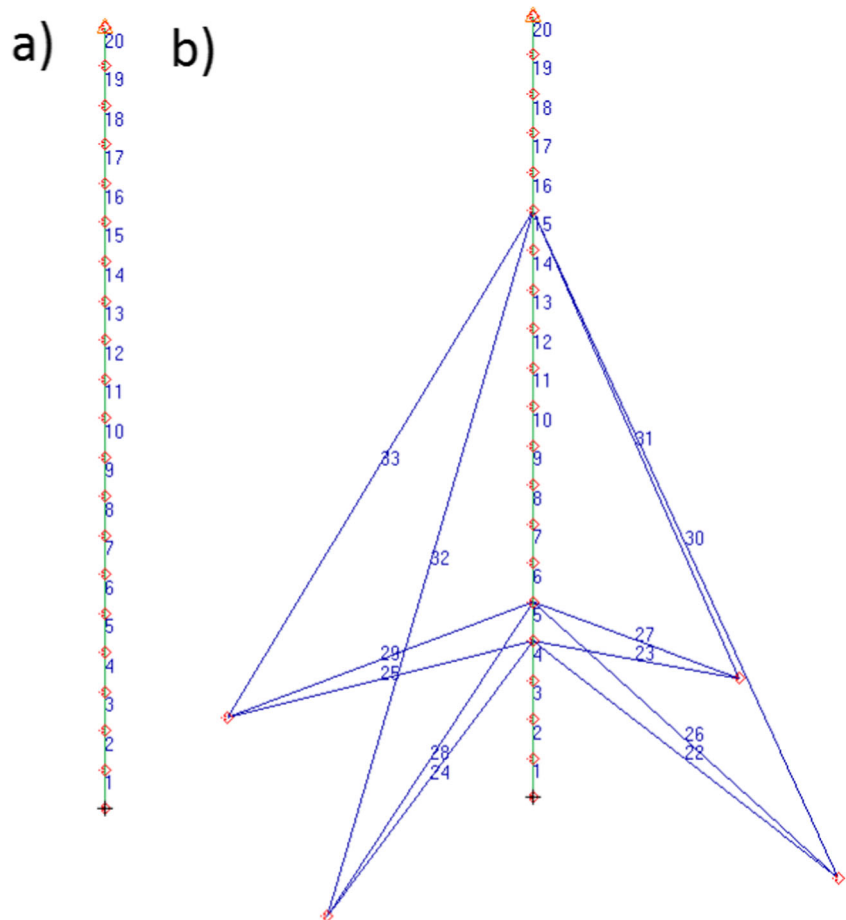
Fig. 1 Computation strategy

2.2 Sampling

Sampling is the first step in the optimization loop. The sampling stage is performed automatically, and as a result, a population of variants is created (sampled). Design variables are generated for particular beings in the considered generation based on a given variable’s ranges or juxtapositions (for

discrete values). Sampling is performed using a radial basis function (RBF) network with Hardy multi-quadrics transfer function and a “leave one out” topology selection criterion [40]. The number of variables depends strictly on the adopted assumptions and constraints related to the supporting structure topology and ranges from 3 (simple tubular-type tower) to 8 (guyed mast with 3 guy-wire levels).

Fig. 2 FE model overview and statistics for different topology variants: (a) tubular tower (20 finite elements), (b) guy-wired mast (23–32 finite elements)



Description	Name	Type	Value
Rated power	P_r	constant	3000 [W]
Rated wind speed	v_r	constant	12 [m/s]
Rotor diameter	d_r	constant	3200 [mm]
Rotor swept area	A	constant	8.05 [m ²]
Blade length	l_b	constant	1500 [mm]
Nacelle weight	m_n	constant	75 [kg]
Rated angular velocity	n_r	constant	350 [rpm]
Generator efficiency (PMG)	e_g	constant	90 [%]

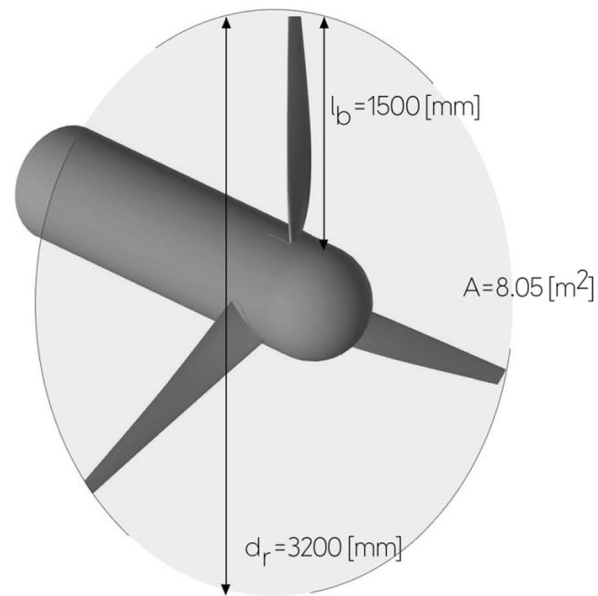


Fig. 3 Small wind turbine model overview (CAD)

At this point, sampling constraints are also applied. For example, the highest guy-wire level cannot pose a threat of colliding with the rotor; therefore, the distance between the guy-wire attachment node and the rotor axis should not be shorter than the blade length.

2.3 Pre-processing

In the second phase, a finite element (FE) model creation procedure is performed automatically using simple scripts and macros for commercially available software [41]. The operations in this stage are based on the variables sampled in the previous step.

First, the model topology is established as a set of curves in virtual 3D space representing supporting structure pipes and potential wires. After subsequent geometric discretization, a relatively simple FE mesh is developed. Discretization of each model is based on 2-node 1D elements formulated as general beams (the mast pipe) as well as potential 2-node 1D elements formulated as rods (guy-wires) (Fig. 2). The use of rod elements for guy-wires is a valid option since the optimization parameters determine only the tensile stress in these elements. Finally, the cross-sectional profiles and other properties are defined for those FE models.

At this stage, boundary conditions and loads are applied automatically according to the model assumptions for a

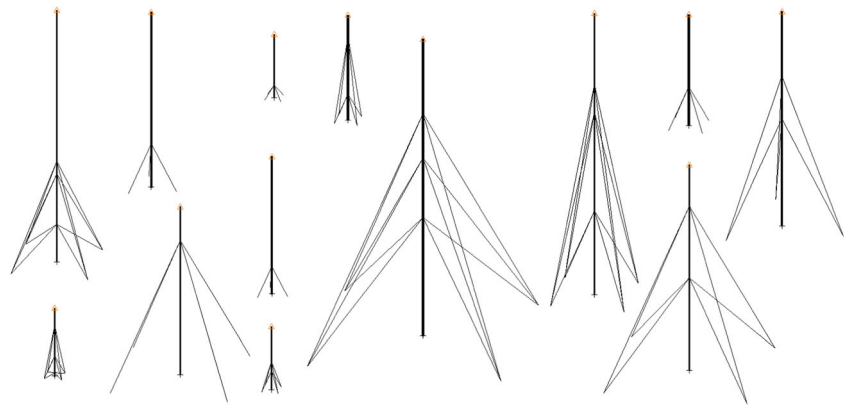
Table 1 Optimization variables set in the example (starting values italicized)

Description	Name	Type	Values
Mast height [mm]	h_{pj}	Discrete	4000; 6000; 8000; 10,000; 12,000; 14,000; 16,000; 18,000; 20,000; 22,000; 24,000; 26,000; 28,000; 30,000
The mast pipe diameter ¹ [mm]	d_{pj}	Discrete	51, 54, 57, 60.3, 63.5, 70, 73, 76.1, 82.5, 88.9, 101.6, 108, 114.3, 127, 133
Number of guy-wires in one level [-]	n_{gwj}	Discrete	3, 4
Number of guy-wire levels [-]	n_{lj}	Discrete	1, 2, 3
1st guy-wire level node [-]	m_{1j}	Discrete	2, 3, 4, 5, 6, 7, 8, 9, 10, 11, 12, 13, 14, 15, 16, 17, 18, 19, 20
2nd guy-wire level node [-]	m_{2j}	Discrete	2, 3, 4, 5, 6, 7, 8, 9, 10, 11, 12, 13, 14, 15, 16, 17, 18, 19, 20
3rd guy-wire level node [-]	m_{3j}	Discrete	2, 3, 4, 5, 6, 7, 8, 9, 10, 11, 12, 13, 14, 15, 16, 17, 18, 19, 20
Guy-wire diameter ² [mm]	d_{gwj}	Discrete	1.8, 2, 2.5, 3, 3.6, 4, 4.5, 5, 5.5, 6, 7, 8

¹ Seamless Steel Pipes and Tubes DIN2448

² Steel Ropes 6×7-NFC (1570 MPa) EN 12385-4

Fig. 4 Randomly selected turbine mast family variants generated by the algorithm (uniform scale and perspective)



chosen design solution. For example, the mast has a joint connection (free rotation in two degrees of freedom (DOFs)), whereas the tubular tower has a fixed connection with the foundation. A potential guy-wire pre-tension is also implemented as a displacement function of the chosen nodes.

The turbine nacelle weight is implemented in the model as a dimensionless mass element at the top of the mast. The whole model is subjected to the gravitational load. The wind drag force acting on the mast pipe applied in every node is calculated using the following drag equation:

$$F_{dj} = C_d \frac{\rho_a \cdot v_j^2 \cdot d_{pj} \cdot l_j}{2} \tag{2}$$

where F_{dj} is the wind drag force per node for variant j , C_d denotes the drag coefficient for cylinder, ρ_a is the air density, v_j is the extreme wind speed for variant j according to the IEC 61400-2 standard, and d_{pj} is the mast pipe diameter for variant j ; and

$$l_j = \frac{h_{pj}}{n_e} \tag{3}$$

where l_j is the node-to-node distance for variant j , h_{pj} is the mast height for variant j , and n_e is a number of FEs for the mast pipe (Fig. 2).

2.4 Coupled aero-servo-elastic numerical simulations

The aerodynamic load resulting from SWT operation is obtained using coupled non-linear numerical simulations in the time domain based on a combination of different models, including aerodynamics, elastic deformation, servo-dynamics, power generation, and control systems [42]. The software is a set of various mathematical models that, due to mutual data exchange (loose and tight coupling schemes) between modules, obtain a solution of the problem in the form of the dynamic response of the system [43]. The algorithm is derived from theory and fundamental laws of physics, with appropriate simplifications and assumptions, and is then enhanced with analytical and numerical solutions as well as experimental data [42]. The wind turbine models in the chosen software are characterized by 24 DOFs. The calculations can therefore

Table 2 Structure constants used in the example

Description	Name	Type	Value
Foundation safety factor	x_{fund}	Constant	2 [-]
Allowable bearing value of soil ¹	σ_{bws}	Constant	0.025 [MPa]
Mast pipe foundation (plate) height to width ratio	x_{fp}	Constant	0.25 [-]
Optimal angle of the highest level of guy-wires	φ_{gw}	Constant	60 [°]
Guy-wire optimal stress ²	σ_{gw}	Constant	0.1 $Rm = 157$ [MPa]
Approximate Young's modulus of guy-wires ²	E_{gw}	Constant	96 [GPa]
The rope compactness factor ²	f_{gw}	Constant	0.38 [-]
Young's modulus of mast pipes	E_p	Constant	210 [GPa]
Poisson ratio of mast pipes	ν_p	Constant	0.33 [-]
Density of mast pipes	ρ_p	Constant	7850 [kg/m ³]
Density of guy-wires ²	ρ_{gw}	Constant	4376 [kg/m ³]
Density of reinforced concrete	ρ_c	Constant	2500 [kg/m ³]

¹ CE-632 Foundation Analysis and Design: Ultimate Bearing Capacity

² A. Noble & Son LTD., Wire rope & strand, section 02

Table 3 Optimization constraints used in the example

Description	Name	Type	Values
Maximal stress in the mast pipe	σ_{p_max}	Constraint	< 70 [MPa]
Maximal stress in guy-wires	σ_{gw_max}	Constraint	< 240 [MPa]
Minimal buckling factor of the mast pipe	x_{p_min}	Constraint	> 2 [-]

be performed almost in real time on modern PCs, making them suitable for the presented optimization methodology.

An induction method is used to determine the aerodynamic forces in discrete beam elements (BEM) at a given time step, taking into account the wind profile, current location, and velocity of the turbine blades [44]. The dynamically stalled flow field (Beddoes-Leishman), blade tip-loss correction (Prandtl model), and tower drag and downwind shadow models are also included.

2.5 FE analyses

Subsequently, a set of static FE analyses is performed to determine the key responses of the structure variants, e.g., maximal stresses in particular components and the minimal buckling factor of the mast. The loads acting on the mast structure come from turbine operation (the results obtained in the previous step), wind drag force, and gravitational load. These three aspects are sufficient for adequate structural analyses of the SWT supporting structure. The most unfavorable load direction (according to the guy-wire tension) is assumed since it is reasonable to seek the structural response under the most unfavorable conditions to ensure safety issues.

FE simulations of design variants are performed using commercially available FE software [41]. The relatively simple FE mesh based on 2-node beam elements and 2-node rod elements permits accurate calculation of bending and buckling issues in the mast pipe as well as the tension in the guy-wires while maintaining an extremely limited number of calculated DOFs, resulting in very fast computation. All analyses are performed in terms of linear static calculations using a standard FE approach [45]. Linear buckling analyses are defined as eigenvalue problem and are performed using the following approach [41]:

$$([K] + \lambda[K_D])\{\phi\} = 0 \quad (4)$$

Table 4 Cost evaluation constants used in the example

Name	Symbol	Type	Value
Energy cost ¹	c_e	Constant	0.6 [€/kWh]
Mast share of the final price of the SWT ²	p_s	Constant	0.2 [-]
Assumed pipe cost	c_p	Constant	2 [€/kg]
Assumed guy-wire cost	c_{gw}	Constant	20 [€/kg]
Assumed foundations cost	c_f	Constant	0.5 [€/kg]

¹ Energy prices in the EU. Eurostat 92/2015–27 May 2015

² ABB SACE, Wind power plants, Technical Application Papers No 13., 2011

where K is the stiffness matrix, K_D is the differential stiffness matrix, λ denotes an arbitrary multiplier for the applied load, and ϕ corresponds to each distinct eigenvector (buckled shape).

2.6 Economic evaluation

The energy produced by an SWT equipped with a particular mast height is estimated based on given wind data. The provided data set can be defined either as the Weibull distribution parameters α and k or as a set of wind speed measurements with a rate of at least 1 h (preferably even 10 min) and covering a period of at least 1 year [46, 47].

In the presented methodology, the meteorological data concerning wind speed are modified as a function of the mast height (of specific variant j) using the wind shear power law:

$$v_{ij}(h_{pj}) = \left(\frac{h_{pj}}{h_{ref}}\right)^\alpha v_i \quad (5)$$

where $v_{ij}(h_{pj})$ is the wind speed for sample i as a function of the mast height for mast variant j , h_{pj} is the mast height of variant j , h_{ref} is the reference height, α is a terrain-dependent parameter, and v_i denotes the wind speed for sample i at the reference height (either given or generated based on the Weibull parameters).

The power output is calculated using the following formula:

$$E_j = \sum_{i=1}^n \begin{cases} \frac{1}{2} A \rho_a \eta(v_{ij}) v_{ij}^3 t & P_r > \frac{1}{2} A \rho_a \eta(v_{ij}) v_{ij}^3 \\ P_r t & P_r \leq \frac{1}{2} A \rho_a \eta(v_{ij}) v_{ij}^3 \end{cases} \quad (6)$$

where E_j is the estimated total energy generated throughout the test period for variant j , n is the number of samples (either given or generated based on the Weibull parameters), t is the sample

Table 5 Aerodynamic model constants used in the example

Name	Symbol	Type	Value
Air density	ρ_a	Constant	1.2 [kg/m ³]
Drag coefficient for cylinder	C_d	Constant	0.45 [-]
Terrain dependent parameter (wind share)	α	Constant	0.16 [-]

duration, $v_{ij}(h_{pj})$ denotes the wind speed for sample i as a function of the mast height for mast variant j , A is the swept area of the turbine model, ρ_a is the air density, $\eta(v_{ij}(h_{pj}))$ denotes the wind turbine efficiency at a given tip-speed ratio (TSR), and P_r is the turbine’s rated power.

2.7 Post-processing

In the post-processing phase, the key responses of the structure are extracted from the FE analysis results, including the maximal equivalent stress (von Mises) in the mast/tower pipe, maximal tension stress in the guy-wires, minimal buckling factor of the mast/tower pipe, and maximal forces in the foundations. These results are compared with the defined constraints to determine the suitability of each variant (e.g., maximal allowable stress or minimal buckling factor).

At this stage, the masses of specific components are also calculated: mast/tubular tower pipe mass, guy-wire mass, and the total mass of foundations for the mast variant.

Finally, the PP, which is the single-objective optimization function, is calculated for each variant (Eq. 7) based on the obtained responses and assumed cost evaluation constants.

$$PP_j = \frac{m_{pj} \cdot c_p + m_{gwj} \cdot c_{gw} + m_{fj} \cdot c_f}{p_s \cdot E_j \cdot c_e} \tag{7}$$

where PP_j is the PP of variant j [years], m_{pj} is the computed mass of the mast pipe for variant j , m_{gwj} is the computed mass of guy-wires for variant j , m_{fj} is the computed mass of foundations for variant j , E_j is the estimated energy production (1 year span) for variant j , and c_p , c_{gw} , c_f , p_s , c_e are given cost-estimation constants (Table 4).

Table 6 Algorithm parameters used in the example

Name	Value
Starting population size	250 [-]
Number of generations (termination criterion)	30 [-]
Mutation distribution	100 [-]
Mutation probability	0.125 [-]
Crossover distribution	10 [-]
Crossover probability	1 [-]
Tournament size	2 [-]
No of elites	2 [-]
Max repeat optimum/generations	0.001 [-]

2.8 Optimization algorithm

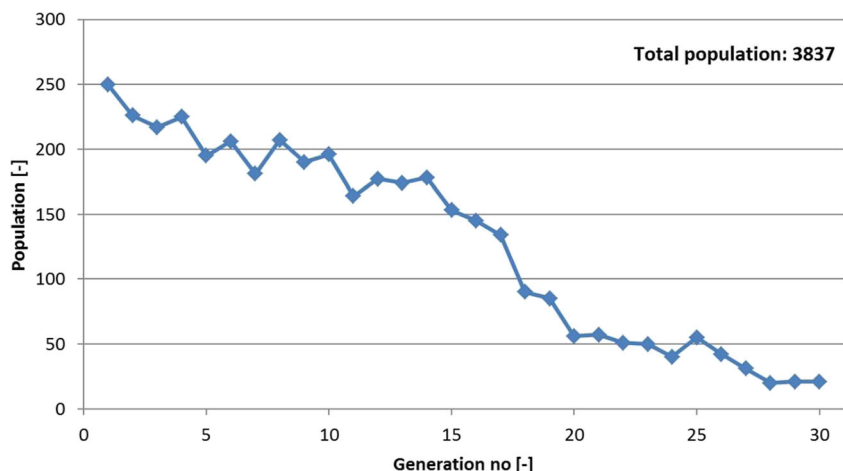
The direct simulation-based single-objective optimization is performed using an evolutionary algorithm [48–51]. Evolutionary algorithms can include processes such as evaluation (objective functions, constraints, and constraint violation of each individual in the parent population), selection performed using the tournament operator (to identify individuals with high fitness and form a mating pool), crossover (the main exploration operator of genetic search; randomly selected parents mate to create children, and these children share the attributes of their parents and thus may be better or worse individuals), mutation (to induce random changes in individuals), and elitism (the process of artificially saving the best individuals) [52]. Because the application of a genetic algorithm is based on probabilistic searching, gradient information is not required, and thus computationally expensive sensitivity analysis steps can be avoided. In general, genetic algorithms are more robust and present better global behavior than mathematical programming methods [53]. Furthermore, genetic algorithms are global optimization techniques that avoid many of the shortcomings of local search techniques on difficult search spaces (which may result in local optima). The power of this approach is derived largely from its ability to efficiently exploit this vast amount of accumulated knowledge using relatively simple selection mechanisms. A genetic algorithm is a probabilistic optimization method; that is, an inferior solution (that may help evolve the correct design variables of the structure) may also have a non-zero probability of participating in the search process [49]. Genetic algorithms exhibit impressive efficiency in practice, although classic gradient search techniques are more efficient for problems satisfying tight constraints [54].

The number of generations is adopted as an optimization criterion. When the defined value is reached, the methodology loop (Fig. 1) is broken, and the results are provided.

3 Exemplary use case

The presented methodology is used to find the optimal supporting structure for an arbitrarily chosen SWT. Additionally, a guyed mast structure is chosen to narrow down the search space for the sake of clarity. Moreover, a mast structure is more representative to illustrate the efficiency of the methodology since it is a relatively more complex structure than a tubular tower.

Fig. 5 Population quantity distribution



3.1 Adopted SWT model

A model of an SWT with a classic three-bladed rotor and a horizontal axis of rotation is adopted for the performed computations (Fig. 3). The physical dimensions and operating parameters of the model are also listed in Fig. 3. The turbine rotor operates in the upwind configuration. The blade geometry is based on the S835, S833, and S834 family of airfoils [55], with a variable chord length and a twist angle. These airfoils are quiet, thick, and natural-laminar-flow and are therefore suitable for SWTs. The generator model has the operating characteristics of a classic synchronous generator equipped with permanent magnets and a variable angular speed [56].

3.2 Input data and adopted parameters

All data presented below are chosen arbitrarily to demonstrate the application of the methodology and should not be considered representative in terms of real design studies on SWT.

Considering the guyed mast structure, there are a total of 8 variables (Table 1). Standardized seamless steel pipes are chosen as a possible material for the mast pipe, and single-layer round-strand ropes are selected as the guy-wires (also from the standard). The sampling variables therefore have discrete values [57]. The guy-wire foundations are predicted to have a mass sufficient to withstand the load without placement underground.

Considering the number of variables and their quantities, there are nearly 58 million possible configurations in this case. It is doubtful that all possible configurations could be calculated to choose the optimal solution. An overview of the randomly selected turbine mast variants sampled according to the data from Table 1 is presented in Fig. 4.

The juxtaposition of structural constants and their arbitrarily chosen values are presented in Table 2. In the presented example, the mast pipe and guy-wire material models are based on Hooke’s theory of elasticity.

The adopted optimization constraints (Table 3) include the maximal stress values of the mast pipe and

Fig. 6 Optimized function (payback period, PP) and its standard deviation during the procedure

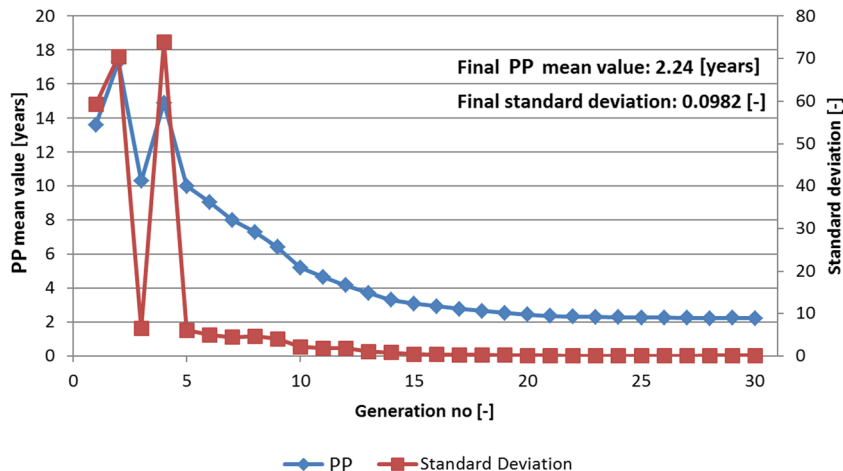
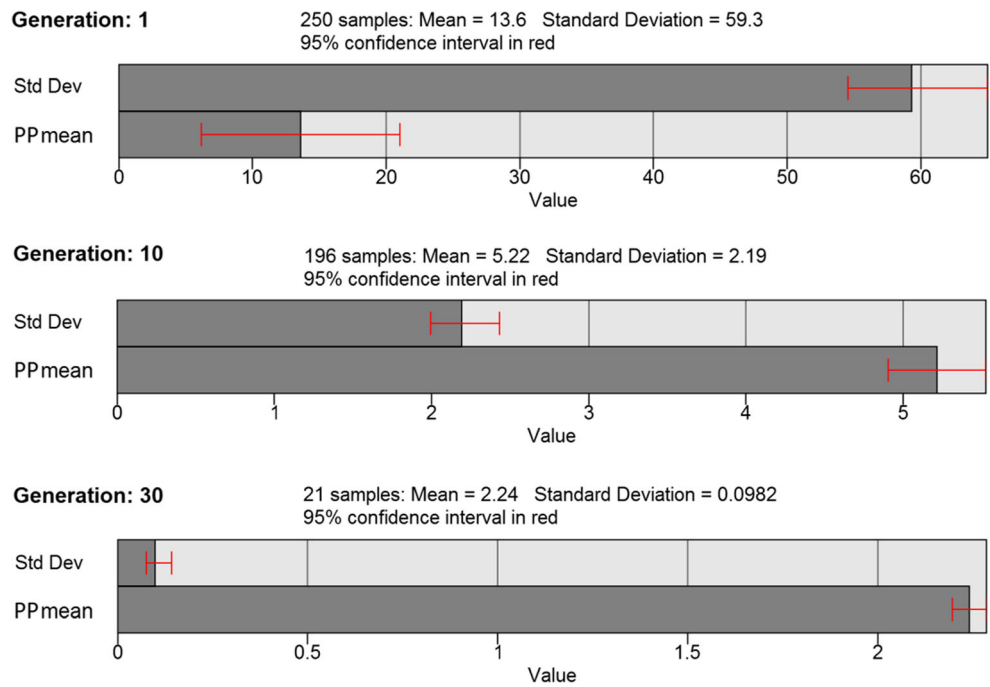


Fig. 7 Statistic summary for the chosen generations



guy-wires as well as the minimal value of the buckling factor provided by the mast structure (as a multiple of the critical buckling force).

The assumed cost evaluation constants are listed in Table 4.

The constants used in the aero-servo-elastic numerical simulations are listed in Table 5.

The meteorological data used in the example is obtained using the Weather Research and Forecasting (WRF) model

[58]. The model is run for each day and for each main synoptic term. Two grids with spatial resolutions of 36 km and 12 km are used. The forecast modeling time is set to 24 h with a 1-h data-sampling rate. The data used in the study cover a period of 1 year (January 01, 2013 to December 31, 2013). Meteorological data are picked for a random location in Poland with typical rural wind speed conditions.

Fig. 8 Optimal solution model appearance

Mast height [mm]	10000
The mast pipe diameter [mm]	76.1
Number of guy-wires [-]	3
Number of guy-wire levels [-]	1
1st guy-wire level node [-]	17
Guy-wire diameter [mm]	3

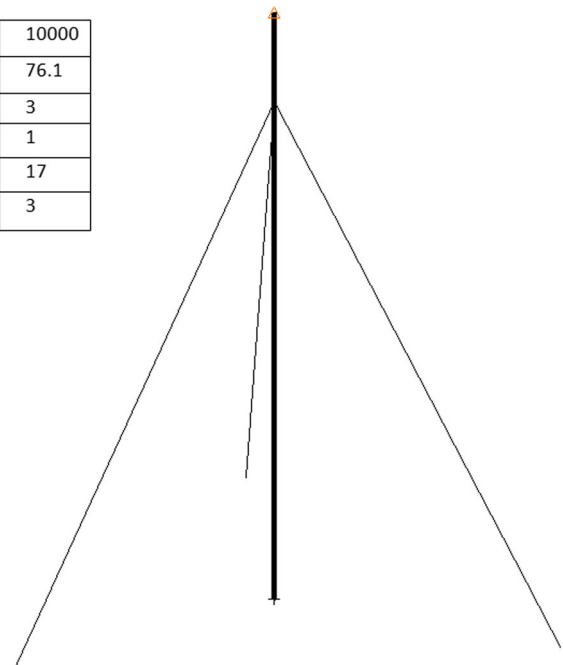


Table 7 Optimal variant key responses

Description	Name	Type	Value
Maximal stress in the mast pipe	σ_{po}	Response	66.7 [MPa]
Maximal stress in guy-wires	σ_{gwo}	Response	227 [MPa]
Buckling factor of the mast pipe	x_{po}	Response	3.45 [-]
Mass of the mast pipe	m_{po}	Response	52.4 [kg] (approx. 104 [€])
Mass of guy-wires	m_{gwo}	Response	0.86 [kg] (approx. 17 [€])
Total mass of foundations	m_{fo}	Response	887 [kg] (approx. 443 [€])
Estimated total energy generated throughout the test period	E_o	Response	2194 [kW]
Payback period (PP)	PP_o	Response	2.15 [years]

The single-objective optimization problem in this example can be expressed as follows:

$$\begin{aligned}
 & \min PP_j(h_{pj}, d_{pj}, n_{gwj}, n_{lj}, m_{1j}, m_{2j}, m_{3j}, d_{gwj}) \\
 \text{subject to } & \left. \begin{aligned}
 & \sigma_{pj}(h_{pj}, d_{pj}, n_{gwj}, n_{lj}, m_{1j}, m_{2j}, m_{3j}, d_{gwj}) < \sigma_{p_max} \\
 & \sigma_{gwj}(h_{pj}, d_{pj}, n_{gwj}, n_{lj}, m_{1j}, m_{2j}, m_{3j}, d_{gwj}) < \sigma_{gw_max} \\
 & x_{pj}(h_{pj}, d_{pj}, n_{gwj}, n_{lj}, m_{1j}, m_{2j}, m_{3j}, d_{gwj}) > x_{p_min}
 \end{aligned} \right\} \quad (8)
 \end{aligned}$$

The optimization algorithm parameters are presented in Table 6.

4 Results and discussion

The full calculation run (30 generations) has a wall time of approximately 4 h on a standard desktop PC. Time-consumption analyses reveal that most of the computation time is spent on file reading and writing operations; therefore, the procedure performance could be significantly improved by using a solid-state drive memory device instead of a hard disk drive.

The total population of the optimization procedure is 3837 and exhibits an irregular, declining character (Fig. 5) because repeated optimum solutions are excluded from the population count in following generations.

Generally, a stable optimization trend can be observed. The mean value of the optimization function (PP) for each generation tends to an optimum (Fig. 6). Considering the standard deviation of the optimization function, stabilization is achieved after approximately five generations, with relatively low values of this parameter thereafter (Fig. 6). These observations indicate that the optimization procedure is successful or trapped in a local optimum.

A statistic summary for the chosen generations is presented in Fig. 7.

Optimal solution variables are presented in Fig. 8, and optimal solution key responses are presented in Table 7.

The obtained optimal variables do not include any of the boundary values (mast height, mast pipe diameter, guy-wire diameter), and thus it can be assumed that the presumed variable ranges are correct and do not interfere with the optimization procedure.

The maximal stress in the mast pipe and the maximal stress in the guy-wires constraints are well-exploited, whereas the buckling factor of the mast pipe is significantly higher than the assumed minimum. Based on the mass properties of the optimal variant, the main scaling factor for the PP is the total mass of the foundations. This outcome is a direct result of the assumptions made, especially the prediction that the guy-wire foundations have sufficient mass to withstand the load without requiring placement underground.

5 Conclusion

The presented numerical methodology allows optimization of chosen design features of small-scale wind turbines supporting structures. Design features and parameters of the structure are expressed as optimization variables (mast height, mast pipe dimensions, guy-wire topology and diameter). Therefore, it is possible to determine key factors (scaling factors) for particular design case. In the presented example, the scaling factor is the total mass of the foundations.

Optimization process takes into account data from different fields of engineering as well as economic aspects of SWT operation. Specifically, the proposed methodology consists of the following: coupled aero-elastic analysis, finite element analysis, and economical evaluation based on mast geometry and reliable weather condition data, simultaneously. Therefore, the obtained optimal solution can be described as more a real-world solution, not a partial solution (e.g., in terms of structural excellence and omitting cost realities).

It is shown that a reasonable computation time and result accuracy can be obtained even for a relatively complicated case (guy-wired masts), thus affirming the choice of modeling simplifications and assumptions.

The described procedure could be easily adopted to different design solutions and a wide range of assumptions and simplifications and hence represents a valuable tool that supports the design process of SWTs.

The scope of future work is to validate the methodology in comparison with a real-world object. The authors have already established a research stand equipped with SWT and sensor equipment and now they are gathering the first sets of data. This approach will allow the identification of potential methodology problems and calibration. The authors will continue subsequently with repeated experiments with statistics on confidence intervals or box plots for greater insight. Ultimately, the authors wish to propose a user application for SWT design and operation planning.

Funding information The study was supported by the Polish-Norwegian Research Programme operated by the National Centre for Research and Development under the Norwegian Financial Mechanism 2009–2014 in the frame of Project Contract No. Pol-Nor/200957/47/2013.

Open Access This article is distributed under the terms of the Creative Commons Attribution 4.0 International License (<http://creativecommons.org/licenses/by/4.0/>), which permits unrestricted use, distribution, and reproduction in any medium, provided you give appropriate credit to the original author(s) and the source, provide a link to the Creative Commons license, and indicate if changes were made.

Publisher's Note Springer Nature remains neutral with regard to jurisdictional claims in published maps and institutional affiliations.

References

- Gsänger S, Pitteloud JD (2015) Small wind world report summary 2015. WWEA. http://small-wind.org/wp-content/uploads/2014/12/Summary_SWWR2015_online.pdf. Accessed 20 July 2015
- Grijalva S, Umer Tariq M (2011) Prosumer-based smart grid architecture enables a flat, sustainable electricity industry 978-1-61284-220-2/11/\$26.00 ©2011 IEEE
- International Electrotechnical Commission (2013) IEC 61400-2: wind turbines—part 2: small wind turbines. ISBN 978-2-8322-1284-4
- Bukala J, Damaziak K, Kroszczynski K, Krzeszowiec M, Malachowski J (2015) Investigation of parameters influencing the efficiency of small wind turbines. *J Wind Eng Ind Aerodyn* 146: 29–38. <https://doi.org/10.1016/j.jweia.2015.06.017>
- Gasch R, Twele J (2012) Wind power plants: fundamentals, design, construction and operation, 2nd edn. Springer, Berlin ISBN 978-3-642-22937-4
- Srinivas N, Deb K (1994) Multiobjective optimization using nondominated sorting in genetic algorithms. *Evol Comput* 2(3): 221–248. <https://doi.org/10.1162/evco.1994.2.3.221>
- Chehouri A, Younes R, Ilinca A, Perron J (2016) Wind turbine design: multi-objective optimization. *Wind turbines—design, control and applications*, edited by Abdel Ghani Aissaoui and Ahmed Tahor. InTech, Rijeka, Croatia, Chapter 6:121–147. <https://doi.org/10.5772/63481>
- Schwefel H-PP (1993) Evolution and optimum seeking: the six generation. Wiley, Hoboken ISBN 0471571482
- Hajela P, Lin C-Y (1992) Genetic search strategies in multicriterion optimal design. *Struct Optim* 4(2):99–107. <https://doi.org/10.1007/BF01759923>
- Alexandrov NM, Hussaini MY (1997) Multidisciplinary design optimization: state of the art. 80, SIAM, United States. ISBN 978-0898713596
- Deb K (2001) Multi-objective optimization using evolutionary algorithms, vol 16. Wiley, Hoboken ISBN 047187339X
- Muskulus M, Schafhirt S (2014) Design optimization of wind turbine support structures—a review. *J Ocean Wind Energy* 1:12–22
- Chehouri A, Younes R, Ilinca A, Perron J (2015) Review of performance optimization techniques applied to wind turbines. *Appl Energy* 142:361–388. <https://doi.org/10.1016/j.apenergy.2014.12.043>
- Negm HM, Maalawi KY (2000) Structural design optimization of wind turbine towers. *Comput Struct* 74:649–666. [https://doi.org/10.1016/S0045-7949\(99\)00079-6](https://doi.org/10.1016/S0045-7949(99)00079-6)
- Uys PE, Farkas J, Jarmai K, van Tonder F (2007) Optimisation of a steel tower for a wind turbine structure. *Eng Struct* 29:1337–1342. <https://doi.org/10.1016/j.engstruct.2006.08.011>
- Nicholson JC, Arora JS, Goyal D, Tinjum JM (2013) Multi-objective structural optimization of wind turbine tower and foundation systems using isight: a process automation and design exploration software. 10th World Congress on Structural and Multidisciplinary Optimization, 19–24 May 2013, Orlando, Florida, USA
- Yoshida S (2006) Wind turbine tower optimization method using a genetic algorithm. *Wind Eng* 30:453–470. <https://doi.org/10.1260/030952406779994150>
- Yıldırım S, Özkol I (2010) Wind turbine tower optimization under various requirements by using genetic algorithm. *Engineering* 2: 641–647. <https://doi.org/10.4236/eng.2010.28082>
- Blachowski B, Gutkowski W (2016) Effect of damaged circular flange-bolted connections on behaviour of tall towers, modelled by multilevel substructuring. *Eng Struct* 111:93–103. <https://doi.org/10.1016/j.engstruct.2015.12.018>
- Bottasso CL, Campagnolo F, Croce A (2012) Multi-disciplinary constrained optimization of wind turbines. *Multibody Syst Dyn* 27(1):21–53. <https://doi.org/10.1007/s11044-011-9271-x>
- Wang L, Wang T, Wu J, Chen G (2017) Multi-objective differential evolution optimization based on uniform decomposition for wind turbine blade design. *Energy* 120:346–361. <https://doi.org/10.1016/j.energy.2016.11.087>
- Barnes RH, Morozov EV (2016) Structural optimisation of composite wind turbine blade structures with variations of internal geometry configuration. *Compos Struct* 152:158–167. <https://doi.org/10.1016/j.compstruct.2016.05.013>
- Fagan EM, Flanagan M, Leen SB, Flanagan T, Doyle A, Goggins J (2017) Physical experimental static testing and structural design optimisation for a composite wind turbine blade. *Compos Struct* 164:90–103. <https://doi.org/10.1016/j.compstruct.2016.12.037>
- Kusiak A, Zhang ZJ, Li MY (2010) Optimization of wind turbine performance with data-driven models. *IEEE Trans Sustain Energy* 1(2):66–76. <https://doi.org/10.1109/TSTE.2010.2046919>
- Chen J, Shen WZ, Wang Q, Pang X, Li S, Guo X (2013) Structural optimization study of composite wind turbine blade. *Mater Des* 46: 247–255. <https://doi.org/10.1016/j.matdes.2012.10.036>
- Huang J, Yuan Y, Wang Z, Qi Z, Xing C, Gao J (2018) A global-to-local registration and error evaluation method of blade profile lines based on parameter priority. *Int J Adv Manuf Technol* 94:3829–3839. <https://doi.org/10.1007/s00170-017-1125-0>
- Pourrajabian A, Afshar PAN, Ahmadizadeh M, Wood D (2016) Aero-structural design and optimization of a small wind turbine blade. *Renew Energy* 87:837–848. <https://doi.org/10.1016/j.renene.2015.09.002>

28. Vucina D, Marinic-Kragic I, Milas Z (2016) Numerical models for robust shape optimization of wind turbine blades. *Renew Energy* 87:849–862. <https://doi.org/10.1016/j.renene.2015.10.040>
29. Tang X, Huang X, Peng R, Liu X (2015) A direct approach of design optimization for small horizontal axis wind turbine blades. *Procedia CIRP* 36:12–16. <https://doi.org/10.1016/j.procir.2015.01.047>
30. Vitale AJ, Rossi AP (2008) Computational method for the design of wind turbine blades. *Int J Hydrog Energy* 33:3466–3470. <https://doi.org/10.1016/j.ijhydene.2008.04.054>
31. Olasek K, Karczewski M, Lipian M, Wiklak P, Jozwik K (2016) Wind tunnel experimental investigations of a diffuser augmented wind turbine model. *Int J Numer Methods Heat Fluid Flow* 26:2033–2047. <https://doi.org/10.1108/HFF-06-2015-0246>
32. Asl HJ, Yoon J (2016) Power capture optimization of variable-speed wind turbines using an output feedback controller. *Renew Energy* 86:517–525. <https://doi.org/10.1016/j.renene.2015.08.040>
33. Gao R, Gao Z (2016) Pitch control for wind turbine systems using optimization, estimation and compensation. *Renew Energy* 91:501–515. <https://doi.org/10.1016/j.renene.2016.01.057>
34. Ayadi M, Derbe N (2017) Nonlinear adaptive backstepping control for variable-speed wind energy conversion system-based permanent magnet synchronous generator. *Int J Adv Manuf Technol* 92:39–46. <https://doi.org/10.1007/s00170-017-0098-3>
35. Akbar MA, Mustafa V (2016) A new approach for optimization of vertical axis wind turbines. *J Wind Eng Ind Aerodyn* 153:34–45. <https://doi.org/10.1016/j.jweia.2016.03.006>
36. Kear M, Evans B, Ellis R, Rolland S (2016) Computational aerodynamic optimisation of vertical axis wind turbine blades. *Appl Math Model* 40:1038–1051. <https://doi.org/10.1016/j.apm.2015.07.001>
37. Marinic-Kragic I, Vucina D, Milas Z (2018) Numerical workflow for 3D shape optimization and synthesis of vertical-axis wind turbines for specified operating regimes. *Renew Energy* 115:113–127. <https://doi.org/10.1016/j.renene.2017.08.030>
38. Clifton-Smith MJ, Wood DH (2010) Optimisation of self-supporting towers for small wind turbines. *Wind Eng* 34:561–578
39. Deb K (2014) Multi-objective optimization. Search methodologies. Introductory tutorials in optimization and decision support techniques. Springer, Boston, pp 403–449
40. Stander N, Roux W, Basudhar A, Eggleston T, Goel T, Craig K (2014) LS-OPT® user's manual. A Design optimization and probabilistic analysis tool for the engineering analyst. Copyright© LIVERMORE SOFTWARE TECHNOLOGY CORPORATION
41. MSC Software Corporation (2003) MSC.Nastran 2004—reference manual. Printed in USA, ©2003
42. Buhl ML, Manjock A (2006) A comparison of wind turbine aeroelastic codes used for certification. American Institute of Aeronautics and Astronautics. <http://www.nrel.gov/docs/fy06osti/39113.pdf>. Accessed 19 March 2015
43. Brusca S, Lanzafame R, Messina M (2014) Flow similitude laws applied to wind turbines through blade element momentum theory numerical codes. *Int J Energy Environ Eng* 5:313–322. <https://doi.org/10.1007/s40095-014-0128-y>
44. Moriarty PJ, Hansen AC (2015) AeroDyn theory manual. National Renewable Energy Laboratory. <http://www.nrel.gov/docs/fy05osti/36881.pdf>. Accessed 20 March 2015
45. Belytschko T, Liu WK, Moran B (2000) Nonlinear finite elements for continua and structures. Wiley, Chichester, pp 317–337 ISBN 978-1-118-63270-3
46. Bilir L, Imir M, Devrim Y, Albostan A (2015) Seasonal and yearly wind speed distribution and wind power density analysis based on Weibull distribution function. *Int J Hydrog Energy* 40:15301–15310. <https://doi.org/10.1016/j.ijhydene.2015.04.140>
47. Drew DR, Barlow JF, Cockerill TT, Vahdati MM (2015) The importance of accurate wind resource assessment for evaluating the economic viability of small wind turbines. *Renew Energy* 77:493–500. <https://doi.org/10.1016/j.renene.2014.12.032>
48. Holland JH (1975) Adaptation in natural and artificial systems. Univ. Michigan, Ann Arbor
49. Goldberg DE (1989) Genetic algorithms in search, optimization and machine learning. Addison-Wesley Publishing Company, Boston
50. Bendsoe MP, Mota Soares CA (1992) Topology design of structures. Proceedings of the NATO Advanced Research Workshop on Topology Design of Structures, Sesimbra
51. Mitsuo G, Runwei C (2000) Genetic algorithms and engineering optimization. Wiley, Hoboken
52. Marler RT, Arora JS (2004) Survey of multi-objective optimization methods for engineering. *Struct Multidisc Optim* 26:369–395. <https://doi.org/10.1007/s00158-003-0368-6>
53. Lagaros ND, Papadrakakis M, Kokossalakis G (2002) Structural optimization using evolutionary algorithms. *Comput Struct* 80:571–589. [https://doi.org/10.1016/S0045-7949\(02\)00027-5](https://doi.org/10.1016/S0045-7949(02)00027-5)
54. Grefenstette JJ (1986) Optimization of control parameters for genetic algorithms. *IEEE Trans Syst Man Cybern* 16(1):122–128. <https://doi.org/10.1109/TSMC.1986.289288>
55. Somers DM (2005) The S833, S834, and S835 Airfoils. Subcontract report. National Renewable Energy Laboratory. https://wind.nrel.gov/airfoils/Documents/S833,S834,S835_Design.pdf. Accessed 20 May 2016
56. Bukala J, Damaziak K, Karimi HR, Malachowski J (2016) Aeroelastic coupled numerical analysis of small wind turbine—generator modeling. *Wind Struct* 23(6):577–594. <https://doi.org/10.12989/was.2016.23.6.577>
57. Grierson DE, Pak WH (1993) Optimal sizing, geometrical and topological design using a genetic algorithm. *Struct Optim* 6:151–159. <https://doi.org/10.1007/BF01743506>
58. Bukala J, Damaziak K, Karimi HR, Kroszczynski K, Krzeszowiec M, Malachowski J (2015) Modern small wind turbine design solutions comparison in terms of estimated cost to energy output ratio. *Renew Energy* 83:1166–1173. <https://doi.org/10.1016/j.renene.2015.05.047>